Pulse-Plated Pb-Sn Alloys from a Methane Sulfonate Electrolyte

(AESF Project 88)

By K.G. Sheppard and Q. Lin

Materials Sci. & Eng., Stevens Institute of Technology, Hoboken, NJ 07030

In AESF Project 88 we have investigated the application of pulse plating to electrodeposited lead-tin solder alloys from methane sulfonate electrolytes. We have shown that the amount of surfactant additive needed to suppress dendritic growth can be reduced by an order of magnitude compared to D.C plating. In this paper we describe the mechanical properties of the pulse plated solder alloys, both before and after reflow. The tensile behavior was measured using a mini-tensile tester developed at Stevens under previous AESF sponsorship.

Introduction

Electrodeposition of lead-tin solder alloys is important in a variety of electronic packaging applications[1,2]. The fluoborate electrolytes have dominated lead-tin plating technology for many years because of their stability and ability to allow high speed deposition[3]. Concern over environmental impact has resulted in a demand for a less toxic and corrosive electrolyte for lead-tin deposition. Recently, proprietary electrolytes based on sulfonates of lead and tin have been introduced.

As with the fluoborate baths, organic additives are needed to promote desirable deposition characteristics, i.e. dendrite suppression and improved throwing power[4]. The objective of the present study is to evaluate pulse plating as a means to produce uniform deposition characteristics over a wide range of current density while reducing the organic additive requirements.

Pulse-plating, because it provides a measure of control over both mass transport and the crystallization process, offers the possibility of influencing deposit composition and morphology without additives or with significantly reduced additive amounts[5]. Codeposition of impurities can be significantly reduced by pulse-plating, for example in gold[6], because during the off-time desorption from the surface can occur. Pulse plating will influence the deposition process in a manner which will be specific to the particular system being considered.

A further important consideration in electrodeposition that can be influenced by pulse plating is current distribution and hence throwing power and surface roughness. Current distribution is categorized as primary, secondary and tertiary depending on whether it is dominated by electrolyte resistance, activation polarization or a combination of activation and mass transport polarizations respectively. Pulse plating has no influence under primary current distribution and can produce a less desirable distribution than direct current plating under secondary conditions. However, it is tertiary current control that can provide the most desirable current distribution in terms of uniformity. With pulse plating in combination with suitable hydrodynamic conditions it is possible to promote a transition to a tertiary type of distribution by influencing the diffusion layer thickness[7].

Related to the above, the beneficial effects of pulse plating on the distribution of gold deposits plated through a photoresist mask have been described[8]. The incorporation of anodic pulses into the pulse sequence can also have beneficial effects on deposit uniformity[9] and surface roughness.

There has been little published on the pulse-plating of lead-tin alloys and none on deposits from the sulfonate electrolytes. Knodler et al.[10] have investigated the effects of pulse parameters on alloy composition and deposition efficiency from fluoroborate bath. Cheh[11] also studied the effects of pulse plating on composition from a fluoborate bath as experimental verification of a model to predict the composition of pulse-plated alloys. Interestingly he found that the tin dissolves during the off-period while the lead continues to deposit. Chin has used high current pulses to promote localized deposition of solder[12].

Experimental

The electrolyte compositions chosen for the present work were based on the results of previous studies at Stevens in which we investigated the effects of a number of additives and a range of d.c. plating conditions on deposition from methane sulfonate

electrolytes. For many of the experiments to evaluate plating variables, the electrolyte contained 40 g/l Sn (0.34M) and 20.25 g/l Pb (0.1M). This we refer to as the 2:1 tin/lead bath. Other metal ratios in the bath were obtained by reducing the lead content. The solution was made up as follows: 130 ml/l methane sulfonic acid (MSA) (70%); 133 ml/l stannous methane sulfonate (SMS) concentrate; 45 ml/l lead methane sulfonate (LMS) concentrate; the balance was deionized water. The lead concentrate contained 53% LMS, 2% MSA and 45% water. The tin concentrate had 50% SMS, 4-5% MSA and the balance water. The as-supplied SMS concentrate contained < 1% of a proprietary anti-oxidant, identified as a di-hydroxy aromatic. This is required to inhibit oxidation of the Sn^{2+} to Sn^{4+} during storage.

An organic additive was employed in this study, namely reagent grade Triton X-100, 5ml/l (used full strength). This is a proprietary (Rohm and Haas) polymeric non-ionic surfactant with the formula $C_8H_{17}(C_6H_4)(OCH_2CH_2)_xOH$ and average molecular weight of 628. Volumetric additions were used for measurement convenience.

Experiments have been performed to measure the effects of different amounts of Triton-X-100 under pulse-plating conditions at a rotating copper disc electrode. The rotating disc electrode was employed to provide controlled transport. All experiments were conducted at 25°C. The deposit characterization was performed in a JEOL 840 scanning electron microscope euipped with an X-ray energy dispersive analyser. The chemical analysis obtained with the latter was calibrated with pure lead and tin samples.

The mechanical properties of pulse-plated solder deposits were measured with a mini-tensile tester developed at Stevens by R. Weil under past AESF sponsorship. This device is able to provide strength and ductility data on thin films with specimen dimensions scaled down to match the film thickness[13]. Eutectic (60Sn/40Pb) and high lead (10Sn/90Pb) solder compositions were deposited for these measurements. As most solder is subject to reflow (melting) during subsequent component processing, the properties of reflowed material have also been tested. In order to produce reflowed samples having the correct shape for the tensile tester, a reflow furnace with temperature controller and argon atmosphere system was constructed. A reflow sample mold was developed using chemical etching of glass through a photoresist mask that defined the tensile specimen shape. The mold, when covered with a weighted glass microscope slide, allows reflow of the solder tensile test specimens without dimension change caused by surface tension effects.

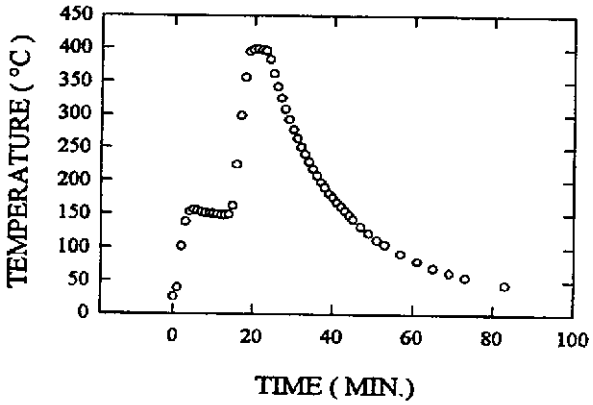

Fig. 1 Reflow temperature profile of Sn/Pb tensile test samples.

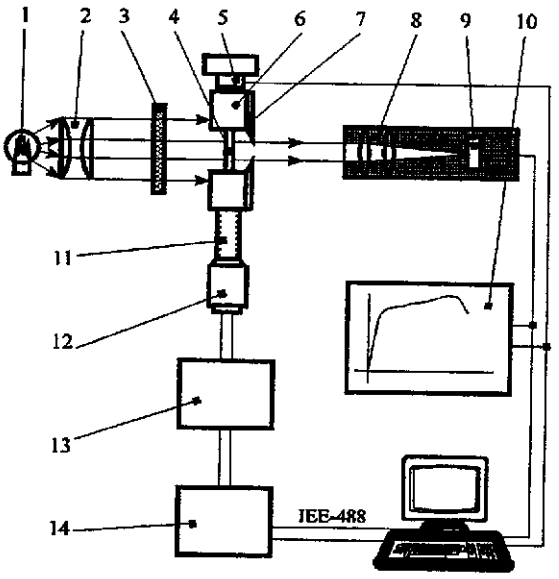

Fig. 2 Computerized mini-tensile test machine.

1. Light Source; 2. Collimating Lenses; 3. Diffuse Screen; 4. Specimen; 5. Load Cell; 6. Grip; 7. Razor Blade; 8. Focusing Lenses; 9. Photo-detector; 10. X-Y Recorder; 11. Load Screw; 12. Stepping Motor; 13. Motor Driver; 14. Indexer.

A reflow temperature profile for the tensile specimens is shown in Fig. 1. Such a temperature profile is used in manufacturing practice. Starting at room temperature, the temperature is raised to 150°C and held at this temperature for 15 minutes. Samples start to melt at about 250°C (eutectic). The peak reflow temperature is about 400°C.

A schematic of the mini-tensile tester is shown in Fig. 2. The amount of light passing between knife edges attached to the specimen grips is used to measure the elastic portion of the tensile curve. This eliminates errors from the elastic distortion of the tensile tester. The larger plastic strains are determined from crosshead displacement. The specimen shape is seen in Fig. 3. This is produced by plating through a photoresist mask onto copper which is subsequently removed by chemical etching. Deposit thickness was approximately 60 μm. The support bar prevents deformation of the gage length during mounting in the grips and is severed just prior to testing.

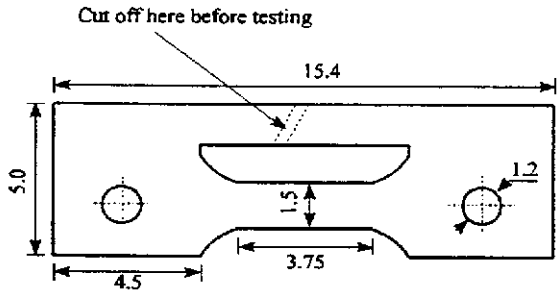

Fig. 3 Schematic of pulse plated Sn/Pb solder alloy tensile test sample. Unit: mm; Total area: 0.667 cm^2; Thickness: 60 μm.

Results and Discussion

Fig. 4 shows how the composition of the d.c. plated alloy varies with current density from approximately 30 to 45% tin in the presence of 5ml/l Triton. It had been found in previous work that 3-5ml/l was the minimum needed to suppress dendritic growth. For d.c. plating the deposit became more grossly nodular as current density was increased. The other curve in Fig. 4 shows the results when pulse plating was employed. It should be noted that these results were obtained with an order of magnitude lower Triton-X concentration in the bath. The tin content is decreased to approximately 10%. Furthermore, there is almost no change in composition over a wide current density range. It should be noted that average current densities, not peak current densities are plotted. The pulse plating produced deposits with good surface morphology (very finely nodular) over the full current density range plotted.

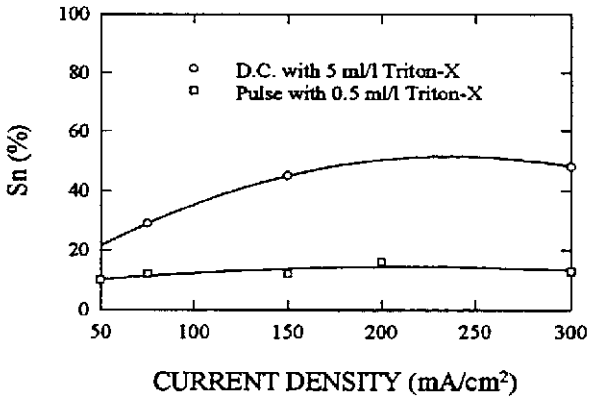

Fig. 4 Effects of average current density on the Sn composition (pulse frequency 100 Hz; duty cycle 10%; Cu disc electrode with 500 rpm).

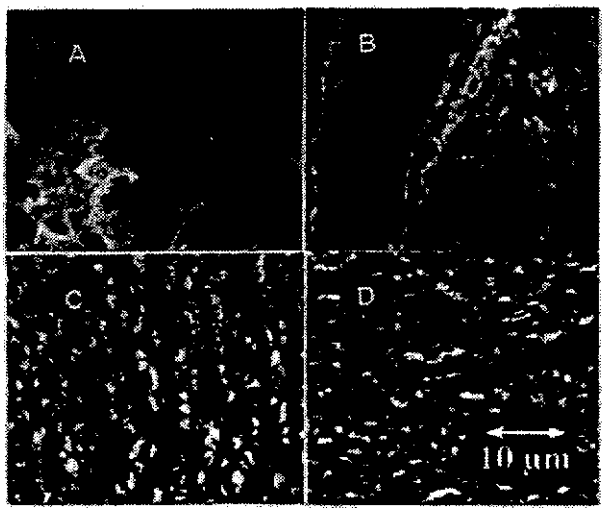

Fig. 5 Effects of Triton-X on the morphology of deposited solder. Sn/Pb (2:1) bath; 75 mA/cm^2; pulse frequency 100 Hz; duty cycle 10%.
(A) no additive; (B) 0.1 ml/l Triton-X; (C) 0.3 ml/l Triton-X; (D) 0.5 ml/l Triton-X.

Pulse plating in the complete absence of the surfactant was not sufficient to completely suppress dendritic growth. Fig. 5A shows a typical morphology. There are no gross dendrites, but at the magnification shown (≈ 1000X) the morphology is clearly dendritic. Adding 0.1 ml/l Triton causes a dramatic change in the dendrite shape (Fig 5B), presumably due to preferential absorption and blockage of certain growth orientations during dendrite branching. The addition of 0.3ml/l Triton is sufficient to completely inhibit the dendrites and little change is observed if more Triton is added. The concentration of Triton needed for full suppression is one tenth of that needed under d.c. plating conditions. Associated with dendrite suppression, a change in deposit composition to much lower tin levels is seen at Triton amounts greater than 0.3 ml/l (Fig. 6). This is to be expected as dendrites are primarily due to tin. However, the tin concentrations are lower than in Triton-suppressed d.c. plating, indicating an additional influence of the pulse plating.

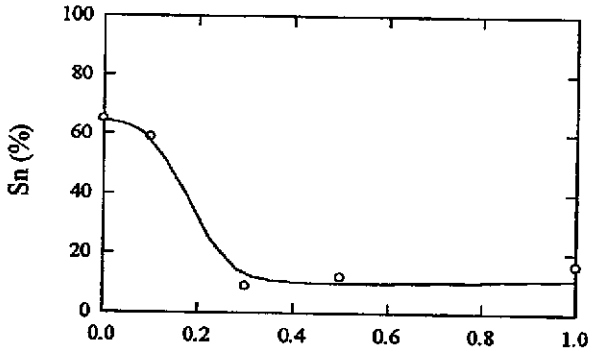

Fig. 6 Effects of Triton-X on the Sn composition of deposited alloy (pulse frequency 100 Hz; 75 mA/cm^2; duty cycle 10%; Cu disc with 500 rpm).

The influence of varying the ratio of tin to lead in the bath for a given set of pulse plating conditions is shown in Fig. 7. Results for d.c plating are included in Fig. 7 for comparison. The pulse plated deposit compositions follow the same trend as those from d.c plating in the presence of the larger Triton concentration. In all cases the pulse plated deposits contained significantly less tin than those from d.c. The morphologies with pulse plating remain good even at high tin content.

Figs. 8 and 9 show the ultimate tensile strength (UTS) for the two compositions, i.e. 60/40 and high lead. The results show that the tensile strength of both alloys is not significantly affected by the average current density used for deposition. Comparing the UTS results at high and low strain rate, the as-plated solder alloys are highly strain rate sensitive. Increase of strain rate from 1.3 x 10^{-3}/sec to 13 x 10^{-3}/sec doubles the ultimate tensile strength of the as-plated alloys. However, such an increase has little effect on the reflowed samples, which have values similar to the as-plated samples tested at the higher strain rate.

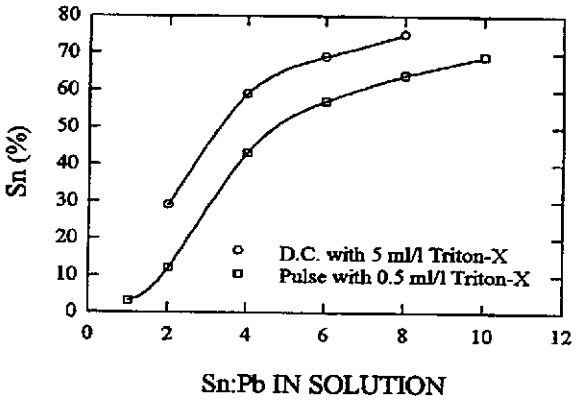

Fig. 7 Effects of solution composition on alloy composition (75 mA/cm^2; duty cycle 10%; frequency 100 Hz; Cu RDE with 500 rpm).

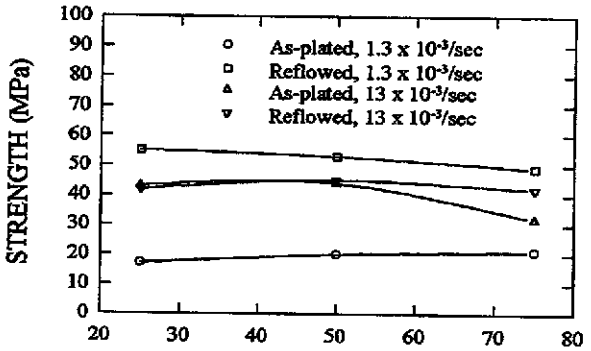

Fig. 8 Effects of average current density on the ultimate tensile strength of 60/ 40 Sn/Pb solder alloy (75 mA/cm^2; duty cycle 10%; frequency 100 Hz; Cu RDE with 500 rpm).

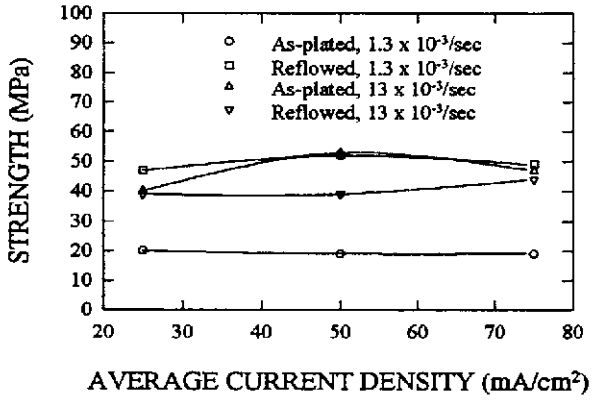

Fig. 9 Effects of average current density on the ultimate tensile strength of 10/ 90 Sn/Pb solder alloy (75 mA/cm^2; duty cycle 10%; frequency 100 Hz; Cu RDE with 500 rpm).

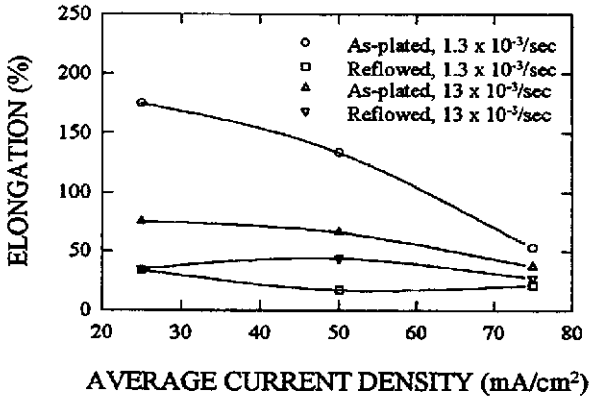

Fig. 10 Effects of strain rate and reflow on the elongation (Sn/Pb 60/40 alloy).

The ductility, as determined from % elongation at failure, is shown in Figs. 10 and 11. Most striking are the very large strains recorded for as-plated material tested at the lower strain rate. This result combined with the low UTS values and strain rate sensitivity, suggests that a degree of superplastic deformation could be occurring at low strain rate. Superplastic behavior is typically associated with a very small grain size. The mechanism is thought to involve grain boundary sliding. The fact that at room temperature lead-tin alloys are at a relatively high homologous temperature (i.e. relative to the melting temperature in °K) means that diffusional processes can enhance grain boundary shear. Large amounts of uniform plastic deformation can then be achieved because the strain rate sensitivity provides a resistance to local necking. Similar superplastic behavior has been reported in fine grained composites made by plating alternating layers of lead and tin[14].

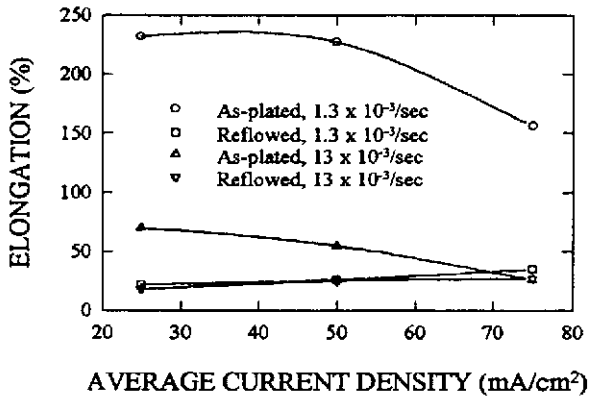

Fig. 11 Effects of strain rate and reflow on the elongation (Sn/Pb 10/90 alloy).

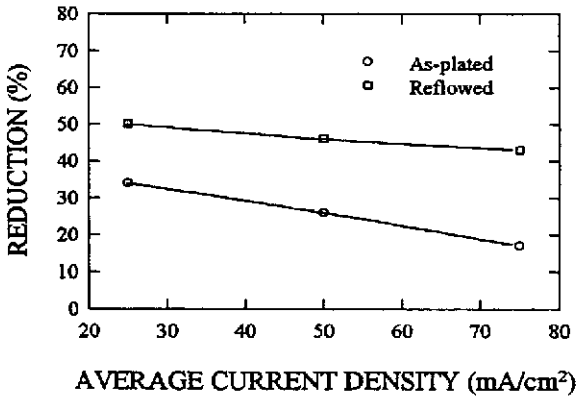

Fig. 12 Effects of average current density on the reduction in cross-section (Sn/Pb 60/40 alloy; strain rate 13 x 10^{-3}).

A second intriguing result is that the ductility of the reflowed material for both alloys, while relatively insensitive to strain rate, is lower than that of the as-plated material. It might reasonably have been expected that melting and solidification would lead to increased grain size and removal of internal defects leading to increased ductility. An explanation for the

results is suggested by Figs. 12-14. Figs. 12 and 13 show the ductility as a percentage reduction in cross-section at the point of fracture rather than as elongation over the gage length. Because of the experimental difficulty, the reductions were estimated from the width change, rather than the true cross-section and therefore probably underestimate the actual reduction in section. It can be seen that by this approach the reflowed samples have greater ductility than as-plated. Thus reflowed material is ductile, however the plastic deformation is highly localized due to the lack of the resistance to necking seen with the as-plated material. The scanning electron microscope photographs of as-plated and reflowed deposits after tensile testing in Fig. 14 clearly shows this difference in necking behavior.

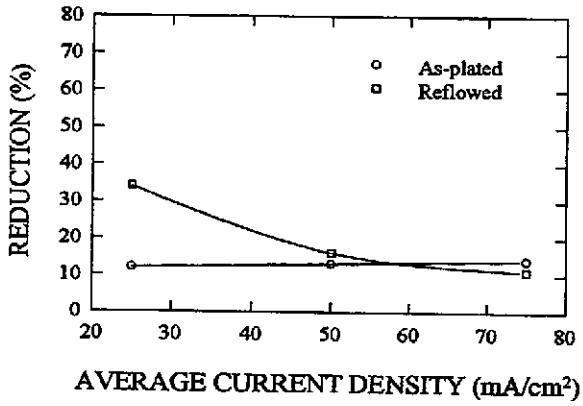

Fig. 13 Effects of average current density on the reduction in cross-section (Sn/Pb 10/90 alloy; strain rate 13 x 10^{-3}).

Conclusions

1. Pulse plating allows deposition of a full range of lead-tin alloys over a wide current density range with good morphology. This is achieved with an additive concentration one tenth that needed to suppress dendritic growth in d.c. plating.

2. As-plated 60Sn/40Pb and 10Sn/90Pb alloys show resistance to necking during tensile testing and thus achieve superplastic levels of elongation.

3. Reflow of the alloys results in material that is more ductile, but only when measured by reduction in area close to the fracture, i.e these materials no longer display resistance to necking and the consequent large elongations.

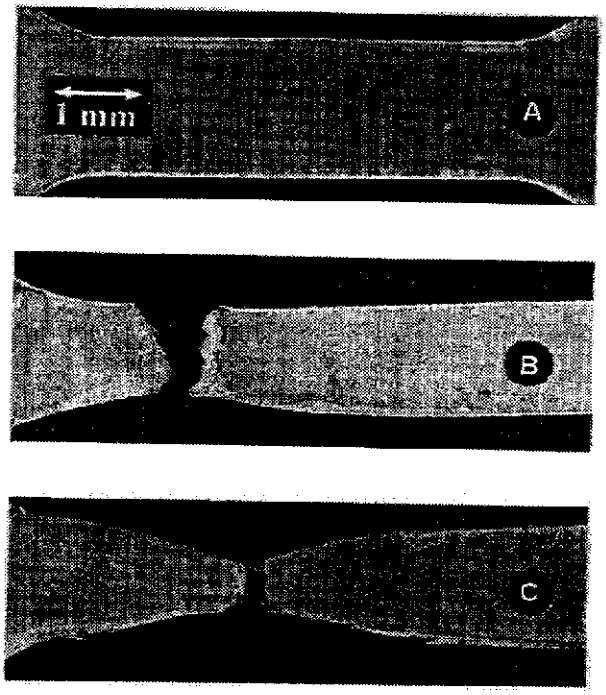

Fig. 14 Photos of tensile test samples.
(A) as-plated;
(B) as-plated and pulled;
(C) reflowed and pulled.

Acknowledgements

We are very grateful to the AESF Research Sponsors and Research Board for supporting this work. We thank Dr. John McCaskie of Atotech USA Inc. (formerly M&T Harshaw) for providing the methane sulfonate concentrates.

References

1. R.K. Asher, *Plating and Surface Finishing*, 75 (1), 34 (1989).
2. E.K. Yung and I. Turlik, *IEEE Trans., Components, Hybrids and Manuf. Techn.*, **14**, 549 (1991).

3. P.A. Kohl, *J. Electrochem. Soc.*, **129**, 1197 (1982): *Plating and Surface Finishing*, **68**, 45 (1981).
4. M. Goodenough and K.J. Whitlaw, *Trans. Inst. Metal Finishing*, **67**, 44 (1989).
5. *Theory and Practice of Pulse Plating*, J.C. Puippe and F. Leaman Eds., American Electroplaters and Surface Finishers Society, Orlando, Florida, 1986.
6. N. Ibl, J.Cl. Puippe and H.F. Angerer, *Surface Technology*, **6**, 287 (1978).
7. O. Chene, M. Datta and D. Landolt, *Oberflache-Surface*, **26**, 45 (1985).
8. J. Horkans and L.T. Romankiw, *J. Electrochem. Soc.*, **124**, 1499 (1977).
9. K.I. Popov, D.C. Totovski and M.D. Maksimovic, *Surface Technology*, **19**, 181 (1983).
10. A. Knodler, Ch.J. Raub and E. Raub, *Metalloberflache*, **39**, 21 (1985).
11. H.Y. Cheh and T. Cheng, in *Electrodeposition Technology, Theory and Practice*, L.T. Romankiw Ed., Proceedings Volume 87-17, The Electrochemical Society, 1987, pp 555-564.
12. D.T. Chin, AESF Project 68.
13. I. Kim and R. Weil, in W.B. Harding and G.A. Dibari(eds.), *Testing of Metallic and Inorganic Coatings*, ASTM STP 947, American Soc. for Testing and Materials, Philadelphia, (1987) p. 11.
14. P.J. Martin and W.A. Backofen, *Transactions of the ASM*, **60**, 352 (1967).